Hindawi
Shock and Vibration
Volume 2018, Article ID 5370438, 8 pages
https://doi.org/10.1155/2018/5370438

Research Article

Resonance Effect Decrease and Accuracy Increase of Piezoelectric Accelerometer Measurement by Appropriate Choice of Frequency Range

Zine Ghemari,[1] **Saad Salah**,[2] **and Rabah Bourenane**[3]

[1]*Electrical Engineering Department, Mohamed Boudiaf University of M'sila, 28000, Algeria*
[2]*LSELM, Badji Mokhtar University, Annaba 23000, Algeria*
[3]*LMI, Mechanical Engineering Department, Badji Mokhtar University, Annaba 23000, Algeria*

Correspondence should be addressed to Zine Ghemari; ghemari-zine@live.fr

Received 19 January 2018; Revised 21 April 2018; Accepted 9 May 2018; Published 27 June 2018

Academic Editor: Miguel Neves

A suitable piezoelectric accelerometer mathematical model is proposed to extract a relationship of motion relative frequency as a function of natural frequency. This relationship helps to select appropriate accelerometer frequency range that minimizes measurement error and improves accuracy. It also allows deducing a formula relating the damping rate and the measurement error of the accelerometer. To protect the accelerometer from failure, the resonance phenomenon effect must be minimized. In order to achieve this objective, physical principle is modeled to find a precise relationship which can determine the accelerometer appropriate frequency range. The developed model was simulated and the obtained results have showed that the selection of the frequency range has minimized the measurement error, increased the accelerometer accuracy, and reduced the resonance effect. Finally a comparative study was conducted to show the importance of the obtained results compared to recent literatures.

1. Introduction

Nowadays, preventive maintenance is the first method used to ensure the operation continuity of electromechanical systems. The conditional preventive maintenance techniques are vibration analysis, acoustic analysis, oil analysis, and thermography. They are designed to monitor industrial plants in operation and detect the appearance of defects.

In reality, the vibration analysis is the most effective technique of conditional preventive maintenance and is widely used in the industry compared to other techniques. This analysis is based on a setup with a vibration sensor (accelerometer) as a main element.

Generally, the accelerometers are placed on the electromechanical systems to convert the mechanical stress or mechanical forces (vibratory movements) into a time electrical signal. The following measurement chain will transform this signal into a frequency electrical signal to facilitate the vibration level measure and give the frequency response to evaluate the system health.

Modeling the accelerometer will allow us to know its physical behavior and convert its operating principle to mathematical equations. The obtained model will make the simulation tests easier and will also improve the accelerometer parameters; thus a new accelerometer design can be proposed.

After discussing the role and the importance of the accelerometer in monitoring and diagnosis field, it is important to focus on improving the characteristics of this instrument particularly the precision, sensitivity, reliability, and availability.

Several reported works [1–4] were carried out on the improvement and development of different types of accelerometers used in monitoring industrial plants.

The work of Jae Min Lee [5] presents the manufacture of a high-shock 2,000 g accelerometer with a plate spring. This accelerometer has high structural stability because it is manufactured such that the plate spring surrounds the mass of the accelerometer. The purpose of Dong-Won Kang et al.

[6] is to accurately predict energy consumption according to physical activity intensity in daily life using an accelerometer.

The problem of determining tilt over various measurement ranges by measuring Cartesian components of the gravity acceleration with application of accelerometers that are Microelectromechanical Systems (MEMS) was discussed in [7].

The method proposed by Jun Ren et al. [8] offers some advantages over available techniques in that additional FRF measurements with different configurations are not needed during the correction process.

Moreover, in the paper of Y-R. Wong et al. [9], the frequency bandwidth of the ZnO accelerometer is extended to its resonance frequency because the measurement of the acceleration is done at the resonance frequency of ZnO accelerometer.

However, in the present work, an expression of the piezoelectric accelerometer natural frequency as a function of the relative frequency of vibratory movements will be extracted in order to reduce the resonance effect on the accelerometer physical behavior and improve measurement accuracy of vibration level.

The main motivation of this work is the appropriate choice of frequency range in order to improve the piezoelectric accelerometer measurement accuracy and reliability. Thus the frequency ratio determined by simulation tests is used to deduce the new equation of damping rate according to measurement error. The proposed equation also allows optimizing the choice of piezoelectric accelerometer parameters and their performances.

Most of previous works were focused on the performances improvements by new designs; in contrast the present work is based on the development of a mathematical model deduced from simulation tests to propose a new design.

2. Piezoelectric Accelerometer

The piezoelectric accelerometer is an instrument of measure attached to a vibrating structure, to measure its acceleration by the conversion of mechanical force (vibratory motion) to a time electric signal. This signal is then transformed to a frequency electrical signal to facilitate finding information on the vibration level. The operation principle of any accelerometer is based on the fundamental law of dynamics [10]:

$$F = m.\gamma \quad (1)$$

It consists of equality between the inertial force of sensor seismic mass and a biasing force applied to the mass. Generally, there are several types of piezoelectric accelerometers. The compression accelerometer type, shown in Figure 1, was the first type to be developed. The shear type, which is arranged so the active element is subjected to shear forces, is generally preferred.

The piezoelectric accelerometer can be considered as the standard vibration transducer for machine vibration measurement. It is designed in different configurations, but the illustration of the compression type serves to describe the operation principle.

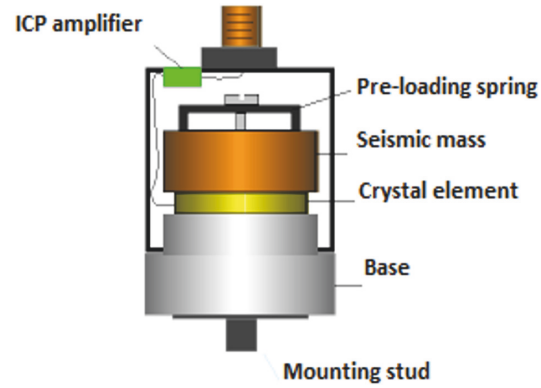

Figure 1: Construction of piezoelectric accelerometer.

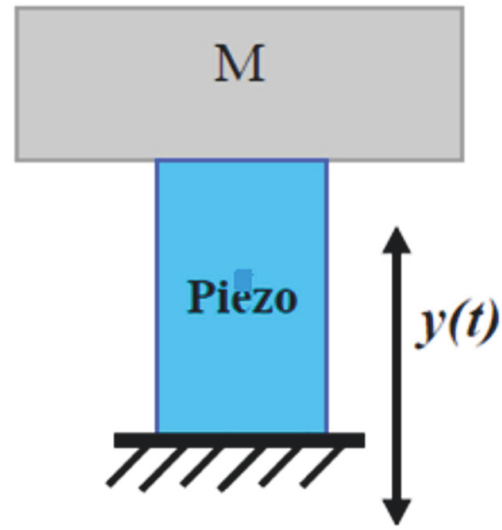

Figure 2: A piezoelectric system.

The seismic mass is clamped to the base by an axial bolt bearing down on a circular spring. The piezoelectric element is squeezed between the mass and the base. When a piezoelectric material experiences a force, it generates an electric charge between its surfaces. There are many such materials, with quartz being one of the most commonly used materials. There are also synthetic ceramic piezo materials that work well and in some cases work at higher temperatures than quartz. If the temperature of a piezo material is increased, finally the so-called "curie point" or "curie temperature" is reached, and the piezoelectric property is lost. Once this happens, the transducer is defective and not repairable.

3. Analytical Approach of Piezoelectric Accelerometer Model

The model design is through analytical description using ordinary differential equations, by developing relations between system variables and model.

The variables depend naturally on their changes over time depending on structures and materials used. In order to construct the analytical model, the system differential equations are developed for one-dimensional structure presented in Figure 2. From (2) and (3), the piezoelectricity is constituted which is given below [10]:

$$\delta = \left(\frac{\sigma}{Y}\right) + dE \quad (2)$$

$$D = d\sigma + \varepsilon E \quad (3)$$

δ is the deformation in the direction of applied force.
σ is the applied mechanical stress ($N.m^{-2}$).

E is the electric field ($V.m^{-1}$).

D is the electric displacement ($C.m^{-2}$).

Y is the elasticity modulus ($N.m^{-2}$).

d is the piezoelectric coupling coefficient ($C.N^{-1}$).

ε is the dielectric constant of the piezoelectric material ($F.m^{-1}$).

For application to a one-dimensional pressure in PZT, there are two polarization direction modes:

(i) Mode 33 or transverse mode

(ii) Mode 31 or vertical mode.

The electromechanical coupling coefficient d33 of PZT is 2 to 3 times greater than d31. A beam structure in mode 33 with interdigitated electrodes is used to obtain a higher electrical efficiency for the sensitivity function. In addition, the equivalent capacitance of the PZT structure which affects the output voltage improves the circuit design of the energy storage.

In order to build the PZT at microstructure base, a thin layer PbTiO3 (PT) is used as an absorber layer to obtain a better adhesion with the substrate. The PZT at microsystem base is focused on beams of PZT/PT/SiO2/Si with interdigitated electrodes where the silicon is designed as seismic mass (Figure 3).

4. Piezoelectric Accelerometer Mechanical Model

To protect the accelerometer from failure, resonance phenomenon effect must be minimized. To achieve this objective, physical principle is modeled to find a precise relation which can determine the appropriate frequency range of the accelerometer.

The operation principle of the piezoelectric accelerometer is based on the direct effect of the piezoelectric material. The deformation of this material caused by external forces generates an electrical signal allowing the measurement of the vibration level.

In general, the accelerometer is considered as a mass **m** mounted at the end of a beam producing a spring stiffness **k** and a damper providing a friction coefficient **c.**

The equation of motion is given as follows:

$$m\ddot{z}(t) + c\dot{z}(t) + kz(t) = -m\ddot{y}(t) \quad (4)$$

z(t) is the displacement.

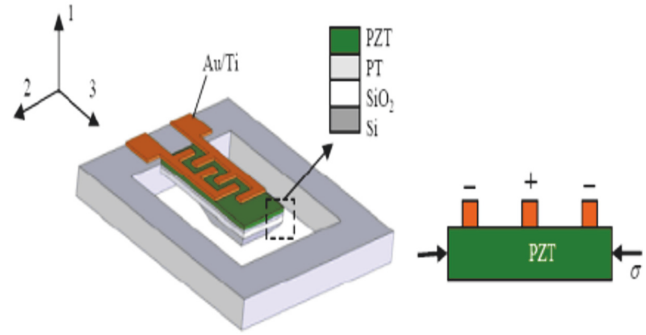

Figure 3: Accelerometer diagram using mode 33 in piezoelectric effect [10].

By applying Laplace transform, the equations below are found:

$$\left(ms^2 + cs + k\right)Z = -ms^2Y \quad (5)$$

$$\left[\frac{Z}{Y}\right] = \frac{-ms^2}{\left(ms^2 + cs + k\right)} \quad (6)$$

Here

$$\omega_n = \left(\frac{k}{m}\right)^{1/2} \quad (7)$$

ω_n represents the accelerometer natural frequency.

The damping rate ξ is given by the following formula:

$$\xi = \frac{c}{(2m\omega_n)} \quad (8)$$

Substituting (8) into (6), the equation below is obtained:

$$\left[\frac{Z}{Y}\right] = \frac{-s^2}{\left(s^2 + 2\xi\omega_n s + {\omega_n}^2\right)} \quad (9)$$

Substituting $s = j\omega$, the magnitude of the system transfer function is expressed as

$$\left[\frac{Z}{Y}\right] = \frac{\omega^2}{\left(-\omega^2 + 2j\xi\omega\omega_n + {\omega_n}^2\right)} \quad (10)$$

Multiplying the denominator of (10) by ${\omega_n}^2/{\omega_n}^2$, we obtain

$$\left[\frac{Z}{Y}\right] = \frac{\omega^2}{\left[{\omega_n}^2\left(1 - (\omega/\omega_n)^2 + 2j\xi\omega/\omega_n\right)\right]} \quad (11)$$

$$Z = \frac{\omega^2 Y}{{\omega_n}^2\left[1 - (\omega/\omega_n)^2 + (2j\xi\omega/\omega_n)\right]} \quad (12)$$

This equation is a complex number; the modulus is given by the equation below:

$$Z = \frac{\omega^2 Y}{\left[{\omega_n}^2\left(\left(1 - (\omega/\omega_n)^2\right)^2 + (2\xi\omega/\omega_n)^2\right)^{1/2}\right]} \quad (13)$$

where Z is the displacement.

Table 1: Parameters of piezoelectric accelerometer.

Parameters	value
Natural frequency (Hz)	2000
Damping rate	0.65, 0.68 and 0.8
Movement amplitude (mm)	0.15

The measurement error is usually defined as the ratio between the measured acceleration (d^2Z/dt^2) and the absolute acceleration (d^2Y/dt^2).
Equation (13) can be written in the following form:

$$Z\omega_n{}^2 = \frac{\omega^2 Y}{\left[\left(\left(1-(\omega/\omega_n)^2\right)^2 + (2\xi\omega/\omega_n)^2\right)^{1/2}\right]} \quad (14)$$

The absolute acceleration of the motion is given by the following expression:

$$\frac{d^2Y}{dt^2} = \omega^2 Y \quad (15)$$

If a piezoelectric accelerometer is chosen such that $\omega/\omega_n \ll 1$ to decrease the error to a minimum value, then (13) becomes

$$Z\omega_n{}^2 = \omega^2 Y \approx \frac{d^2Y}{dt^2} \quad (16)$$

The relative acceleration can be written as

$$\frac{d^2Z}{dt^2} = \omega_n{}^2 Z \quad (17)$$

Hence, the accelerometer measurement error can be expressed as follows:

$$E = \frac{\left(d^2Z/dt^2\right)}{\left(d^2Y/dt^2\right)} - 1 = \frac{\left(Z\omega_n{}^2\right)}{\left(Y\omega^2\right)} - 1 \quad (18)$$

So

$$E = \frac{1}{\left[\left(1-(\omega/\omega_n)^2\right)^2 + (2\xi\omega/\omega_n)^2\right]} - 1 \quad (19)$$

E is defined as accelerometer measurement error.

The developed model must be simulated to see the influence and the importance of frequency range choice in the protection of piezoelectric accelerometer. So, the appropriate choice of frequency range requires an optimum level of sensor protection.

5. Simulation of the Developed Model

The only way to avoid the resonance phenomenon is to have an accelerometer with a very high natural frequency; this will make the resonance frequency difficult to reach. Unfortunately, this is not all the time possible, and in our case for cost reasons this is not an economical alternative. The objective of this work is to decrease the effects of resonance rather than trying to remove it.

From the obtained results we can extract a relationship between resonance frequency and relative frequency of the vibration movement. Then, through this relation an appropriate frequency range can be selected.

The appropriate choice of damping rate improves greatly the parameters of the accelerometer; thus, a new design can be proposed. In the present work, the damping rate value is chosen equal to 0.68; then the obtained results will be compared to the results of the literature [11, 12] conducted with damping rate values equal to 0.65 and 0.7, respectively.

The reason of varying the frequency from 0 at 1500Hz and from 0 at 3000Hz in the simulation tests is to show the influence of resonance phenomenon on piezoelectric accelerometer operation.

The piezoelectric accelerometer parameters used to simulate the developed model are summarized in Table 1.

5.1. Resonance Case. To simulate the displacement and the measurement error as a function of motion relative frequency for the three selected damping rate values (0.65, 0.68, and 0.7) in resonance case, the relative frequency must be varied from 0 to 3000Hz. The following two figures show the obtained simulation results.

Figures 4 and 5 show that the accelerometer loses its operation as the measurement error is larger (between 40 and 50% for a frequency equal to 2000 Hz and more than 65% for a frequency equal to 2500 Hz for all three damping rates); this has affected negatively the accelerometer response.

In order to avoid the resonance effect, further simulation tests based on the variation of relative frequency of vibration motion were conducted. These tests were undertaken with three relative frequency margins varied from 0 to 1500Hz, then from 0 up to 1000Hz, and finally from 0 up to 750Hz.

5.2. Case Where the Relative Frequency Is Varied from 0 to 1500Hz. The simulation results when relative frequency is varied from 0 to 1500Hz are illustrated in Figures 6 and 7.

According to Figure 6, it can be observed that there is a difference between the three displacement curves as a function of the relative frequency for the three selected damping rates. This difference implies the choice influence of damping rate on the piezoelectric accelerometer response.

Figure 7 illustrates the measurement error as a function of relative frequency for three damping rates in the case when the relative frequency is varied from 0 to 1500Hz. A decrease in the measurement error is noted compared to the resonance

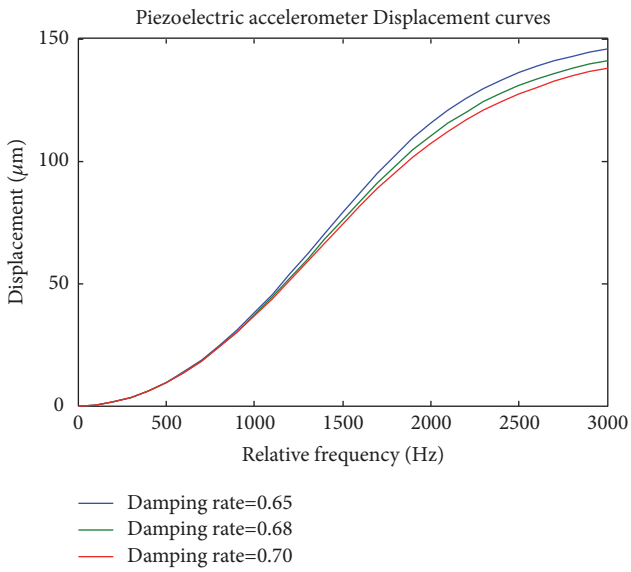

Figure 4: Displacement as a function of relative frequency for three values of damping rate in the resonance case.

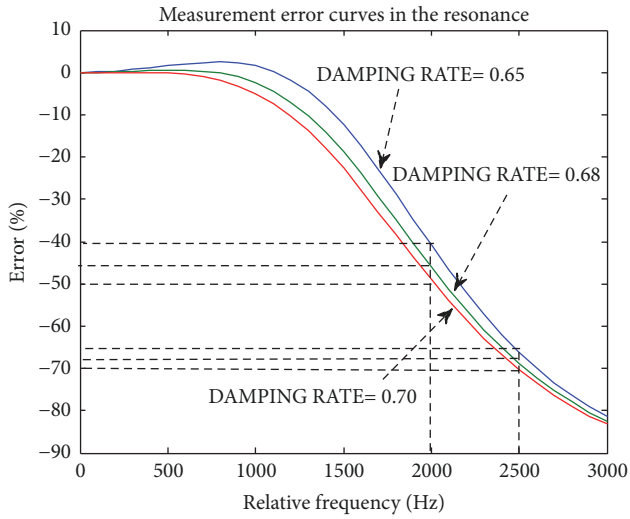

Figure 5: Measurement error as a function of relative frequency for three values of damping rate in the resonance case.

case where the measurement error decreases to a value lower than 25%.

5.3. Case Where the Relative Frequency Is Varied from 0 to 1000Hz. When the relative frequency is varied from 0 to 1000 Hz, the simulation results are presented in Figures 8 and 9.

Figure 8 shows the displacement as a function of relative frequency when the variation is limited between 0 and 1000Hz. It can be seen that the difference between the three displacement curves is reduced compared to the previous case.

Figure 9 illustrates three curves of measurement error based on the relative frequency for three values of damping rate (0.6, 0.68, and 0.70); it can be observed that the measurement error is further reduced compared to the previous case (a value less than 6%).

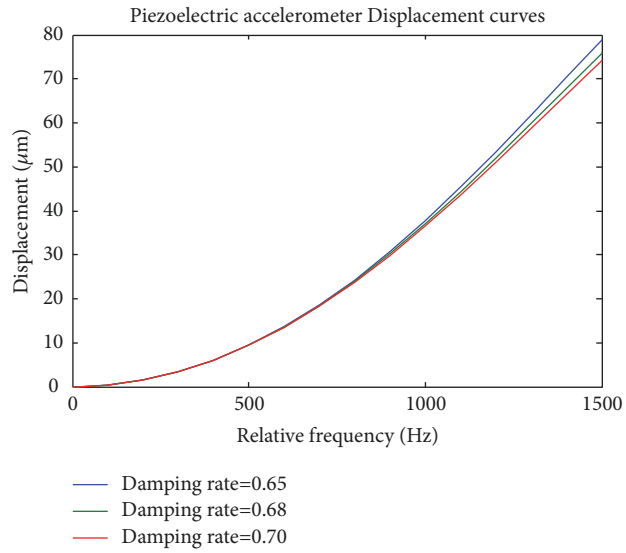

Figure 6: Displacement as a function of relative frequency for three values of damping rate in the case where the relative frequency is varied from 0 to 1500Hz.

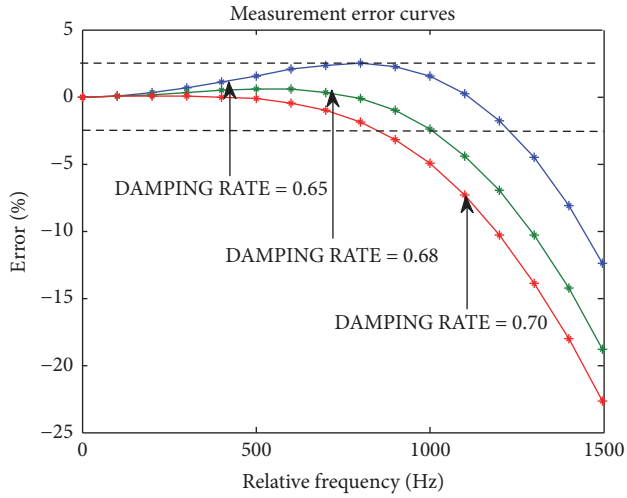

Figure 7: Measurement error as a function of relative frequency for three values of damping rate in the case where the relative frequency is varied from 0 to 1500Hz.

5.4. Case Where the Relative Frequency Is Varied from 0 to 750Hz. When the relative frequency is varied from 0 to 750 Hz, the simulation results are presented in Figures 10 and 11.

It can be noted from Figure 10 that the three displacement curves as a function of the relative frequency are closer to each other. It can be concluded that when the relative frequency is varied from 0 to 750Hz a good frequency margin is reached and accurate response of piezoelectric accelerometer is obtained.

Figure 11 shows the measurement error as a function of relative frequency when this frequency is varied from 0 to 750Hz for three damping rates. It can be seen that the measurement error in this case is highly reduced compared to previous cases. It can be deduced from this figure that the frequency range of this case is the best compared to previous

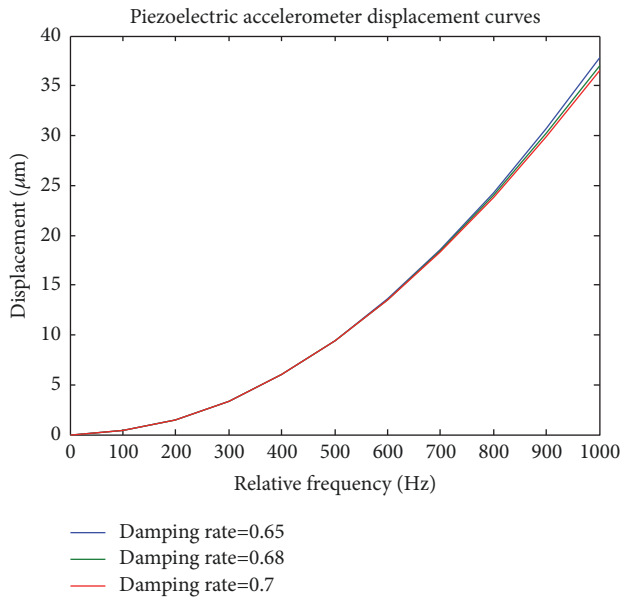

Figure 8: Displacement as a function of relative frequency for three values of damping rate in the case where the relative frequency is varied from 0 to 1500Hz.

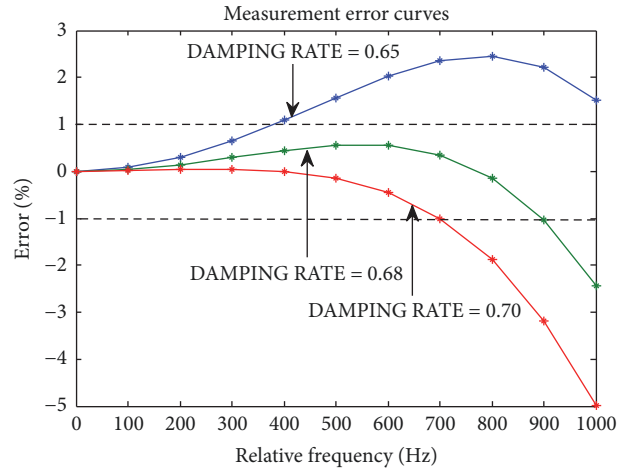

Figure 9: Measurement error as a function of relative frequency for three values of damping rate in the case where the relative frequency is varied from 0 to 1000Hz.

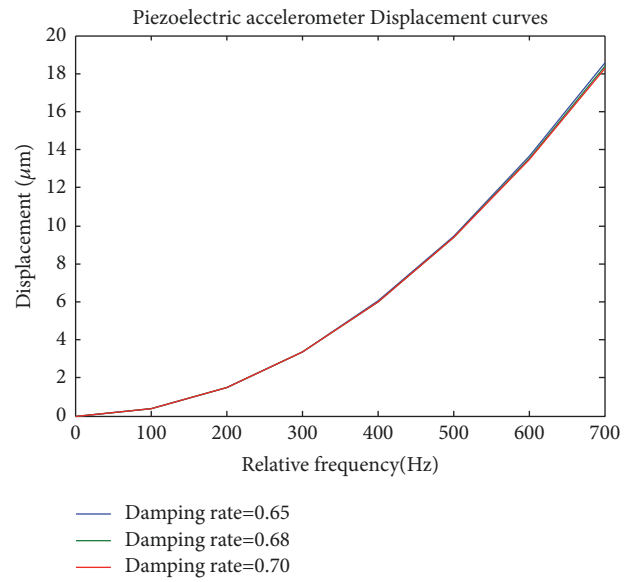

Figure 10: Displacement as a function of relative frequency for three values of damping rate in the case where the relative frequency is varied from 0 to 750Hz.

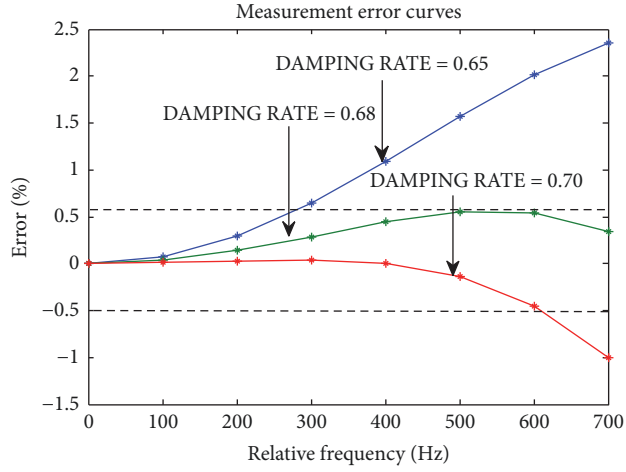

Figure 11: Measurement error as a function of relative frequency for three values of damping rate in the case where the relative frequency is varied from 0 to 750Hz.

cases and the damping rate of 0.68 limits the measurement error to a value of 0.5%.

If the maximum value of relative frequency is taken equal to 800Hz, then the relationship between the motion relative frequency and the natural frequency of accelerometer is as follows:

$$\frac{\omega_{\max}}{\omega_n} = \frac{2}{5} \tag{20}$$

So, we can extract the frequency range by the following relationship:

$$\omega \leq \frac{2\omega_n}{5} \tag{21}$$

This new equation allows selecting the frequency range suitable for piezoelectric accelerometer. This choice aims to minimize the measurement error, increases the accelerometer accuracy, and reduces the resonance effect.

6. Damping Rate New Equation

The frequency ratio determined by simulation tests is illustrated in (16), substituted in (14) to deduce the new equation of damping rate according to the measurement error.

To extract the formula of damping rate as a function of measurement error, we take the maximum value of relative

Table 2: Results comparison of three piezoelectric accelerometers.

Parameters	Accelerometer of Ref [12]	Accelerometer of Ref [13]	proposed Accelerometer
Damping rate	0.8	0.787	0.68
error %	≤ 9%	≤ 8.3%	≤ 1%
Precision %	≥ 91%	≥ 91.7%	≥ 99%

frequency $\omega = 2\omega_n/5$ and replace it in (14); then the following expression is obtained:

$$E + 1 = \frac{1}{\left(1 - \left(\omega/\omega_n\right)^2\right)^2} + \left(\frac{2\xi\omega}{\omega_n}\right)^2) = \frac{1}{\left(0.6988 + 0.633\xi^2\right)} \quad (22)$$

By simplification, it is possible to write

$$(E + 1) * \left(0.6988 + 0.633\xi^2\right) = 1 \quad (23)$$

The equation becomes

$$\left[\frac{1}{(E + 1)}\right] - 0.6988 = 0.633\xi^2 \quad (24)$$

So the damping rate is

$$\xi = \left[\left(\frac{1}{0.633\,(E + 1)}\right) - 1.104\right]^{1/2} \quad (25)$$

Equation (25) shows the new expression of damping rate as a function of measurement error. With this equation it will be easier to find the damping rate for a desired measurement error value.

In order to limit the measurement error to 1% (0.01), the value of damping rate is equal to 0.68 obtained by substitution in (25).

The simulation of this new equation (see (25)) is shown in the Figure 12. In order to simulate this equation, we vary the measurement error from 0 to 10% to see the damping rate variation as a function of piezoelectric accelerometer measurement error.

This new equation makes the optimization of the piezoelectric accelerometer performances easier by choosing appropriate frequency margin to reduce and limit the measurement error to 1% and improve the accelerometer measurement accuracy to a value of 99%.

It is concluded that, for a measurement error of 1%, the accelerometer precision is 99% according to the following equation:

$$P + E = 1 \quad (26)$$

Here P is defined as accelerometer measurement precision.

7. Comparative Study on Three Piezoelectric Accelerometers

Three piezoelectric accelerometers are compared; the first and the second are taken from [12, 13] because of their importance in the field of sensor technology and their new designs. The third accelerometer is the accelerometer proposed in the present work. The damping rates of these accelerometers are 0.8, 0.785, and 0.68, respectively.

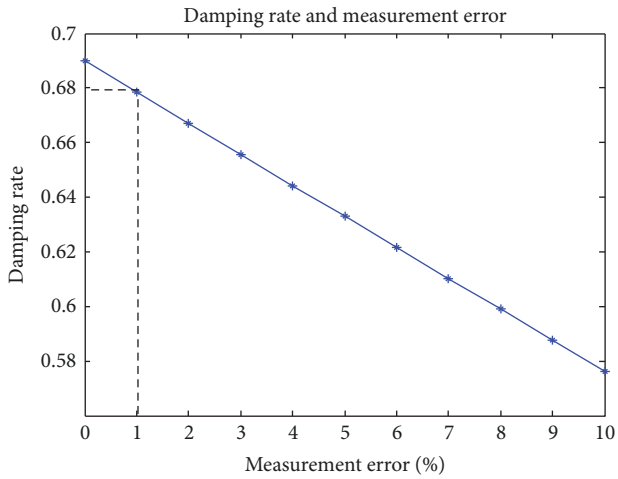

Figure 12: Damping rate as a function of measurement error.

The aim of this study is to illustrate the novelty of this work by comparing the obtained results of the proposed accelerometer with the results of the literature [12, 13].

Two equations (see (20) and (21)) are used to extract measurement error and accuracy for the three accelerometers. The results are summarized in Table 2.

From Table 2, it can be seen that the proposed piezoelectric accelerometer is accurate regarding other two accelerometers (the measurement error does not exceed 1%).

The approach proposed in this paper makes the improvement of piezoelectric accelerometer parameters and performances possible as the methods proposed in the previous works [14, 15]. This method reduces the risk of the resonance phenomenon, protects the accelerometer, improves its accuracy, minimizes its measurement error, and increases its sensitivity.

8. Conclusion

In the present work, a mathematical model of displacement and measurement error of piezoelectric accelerometer is developed. The simulation of this model in the resonance and normal cases has allowed us to deduce a new relationship relating the relative frequency of vibration motion as a function of accelerometer natural frequency. This new relationship is based on selecting appropriate frequency range

of piezoelectric accelerometer which reduces the resonance effect and also allows a deduction of an equation that relates the damping rate to the measurement error.

It is also noted that the damping rate equal to 0.68 limits the measurement error to a value of 0.5% compared to the damping rate selected from the literature.

The obtained results have demonstrated that the selection of appropriate frequency range can minimize the measurement error, increase the accelerometer accuracy, and reduce the resonance effect to protect the accelerometer from failure.

The study has also showed that the proposed piezoelectric accelerometer has better performances than the accelerometers presented in recent works. Finally, a novel piezoelectric sensor can be designed by using the parameters proposed in this work.

In future trends, the accelerometer will be improved by proposing a new model of electrical sensitivity.

Data Availability

The data used to support the findings of this study are available from the corresponding author upon request.

Conflicts of Interest

The authors declare that there are no conflicts of interest regarding the publication of this paper.

Acknowledgments

The authors would like to acknowledge the General Direction of Research and Technological Developments (DGRDT) for the financial support.

References

[1] J. Wang, G. Peng, Z. Hu, H. Yang, and Y. Hu, "Design and analysis of a high sensitivity FBG accelerometer based on local strain amplification," *IEEE Sensors Journal*, vol. 15, no. 10, pp. 5442–5449, 2015.

[2] U. Zabit, O. D. Bernal, and T. Bosch, "Design and analysis of an embedded accelerometer coupled self-mixing laser displacement sensor," *IEEE Sensors Journal*, vol. 13, no. 6, pp. 2200–2207, 2013.

[3] I. Bruant, L. Gallimard, and S. Nikoukar, "Optimization of piezoelectric sensors location and number using a genetic algorithm," *Mechanics of Advanced Materials and Structures*, vol. 18, no. 7, pp. 469–475, 2011.

[4] J. Li, S. Liu, B. Guo, X. Hou, S. Yang, and S. Qiu, "Method for modelling of fluxgate sensor including the geometry influence," *IET Science, Measurement & Technology*, vol. 8, no. 4, pp. 214–219, 2014.

[5] J. M. Lee, C. U. Jang, C. J. Choi et al., "High-shock silicon accelerometer with a plate spring," *International Journal of Precision Engineering and Manufacturing*, vol. 17, no. 5, pp. 637–644, 2016.

[6] D.-W. Kang, J.-S. Choi, J.-W. Lee, and G.-R. Tack, "Prediction of Energy Consumption According to Physical Activity Intensity in Daily Life Using Accelerometer," *International Journal of Precision Engineering and Manufacturing*, vol. 13, no. 4, pp. 617–621, 2012.

[7] S. Łuczak, "Guidelines for tilt measurements realized by MEMS accelerometers," *International Journal of Precision Engineering and Manufacturing*, vol. 15, no. 3, pp. 489–496, 2014.

[8] J. Ren, J. Wang, and S. Bi, "Correction of transducers mass effects from the measured frfs in hammer impact testing," *Shock and Vibration*, vol. 2017, 10 pages, 2017.

[9] Y.-R. Wong, Y. Yuan, H. Du, and X. Xia, "Development of high sensitivity, large frequency bandwidth ZnO-based accelerometers," *Sensors and Actuators A: Physical*, vol. 229, pp. 23–29, 2015.

[10] M. Benmessaoud, *Conception et Modélisation des MEMS: Application aux Accéléromètres [Ph.D. thesis]*, University of Science and Technology of Oran, Algeria, 2014.

[11] M. Thomas, "Étude de l'A.M.E. Analyse Modale Expérimentale," SYS 855 Vibroacoustique, Department of Mechanical Engineering ETS, March 2003.

[12] E. G. Bakhoum and M. H. M. Cheng, "Ultrahigh-sensitivity pressure and vibration sensor," *IEEE Sensors Journal*, vol. 11, no. 12, pp. 3288–3294, 2011.

[13] B. Bais and B. Y. Majlis, "Mechanical sensitivity enhancement of an area-changed capacitive accelerometer by optimization of the device geometry," *Analog Integrated Circuits and Signal Processing*, vol. 44, no. 2, pp. 175–183, 2005.

[14] A. E. Badri, J. K. Sinha, and A. Albarbar, "A typical filter design to improve the measured signals from MEMS accelerometer," *Measurement*, vol. 43, no. 10, pp. 1425–1430, 2010.

[15] A. Albarbar, A. Badri, J. K. Sinha, and A. Starr, "Performance evaluation of MEMS accelerometers," *Measurement*, vol. 42, no. 5, pp. 790–795, 2009.